Volume 1 | Number 1 | Jan 2013 | Pages 1–100

PCCP

Physical Chemistry Chemical Physics
www.rsc.org/pccp

ROYAL SOCIETY OF CHEMISTRY

ROYAL SOCIETY OF CHEMISTRY

www.rsc.org/pccp

Page 1 of 18

Physical Chemistry Chemical Physics
CREATED USING THE RSC LaTeX PCCP ARTICLE TEMPLATE – SEE www.rsc.org/electronicfiles FOR DETAILS

Thermodynamics of Nanoalloys[†]

Florent Calvo[a]

This article reviews recent advances in our understanding of how temperature affects the structure and phase of multimetallic nanoparticles. Focusing on bimetallic systems, we discuss the interplay of size, shape and chemical order on the stable configurations at thermal equilibrium. Besides some considerations about experimental evidences for thermally-induced transformations, most insight is generally provided from theory and computation. The perspectives offered from mesoscopic approaches (i.e. corrected from the bulk) and atomistic simulations complement each other and often allow detailed information about the respective roles of coordination, composition and more generally surface effects to be evaluated. Order-disorder transitions and the melting phase change are strongly altered in nanoscale systems, and we describe how they possibly impact entire phase diagrams.

1 Introduction

The general interest in nanoparticles generally stems from the increase in the surface/volume ratio, which is essential to promote chemical reactivity, but also from indirect consequences of the changes in the band structure associated with the reduction in the number of atoms. Even notions as basic as metallicity itself have been shown to become size dependent in the nanoscale regime, mercury clusters exhibitting for instance van der Waals, then covalent types of chemical bonding before the HOMO-LUMO gap eventually closes after several hundreds of atoms are brought together.[1] Electronic structure directly impacts the optical and magnetic properties, as well as the stable geometries, in the small size regime where 'each atom counts' but also in larger nanoparticles through different surface energies associated with the different crystalline orders and the resulting Wulff shapes.[2]

One way of tailoring the properties of metals as old as metallurgy itself consists of combining different metals into an alloy. Similar ideas have emerged in nanoscience much more recently, probably due to previously uncomplete understanding of pure metal nanoparticles. Nanoalloys, or nanoparticles combining at least two metallic elements, thus play an increasing role in various areas of science and technology owing to the possibility of tuning their properties by varying the composition in addition to size. In the recent years, nanoalloys have found promising applications in areas as diverse as magnetism, optics and plasmonics, catalysis and even life sciences.[3–7]

The potential of nanoalloys in these diverse fields of application originates from the twin influence of size and composition and should be matched with the dual complexity of nanoparticles in general, with their specific size-dependent properties, together with alloys with their composition-dependent properties. One issue of fundamental importance with nanoalloys is that of stability, especially considering the broad variety of synthesis methods based on different physical or chemical techniques and that can produce essentially identical compounds both in size and composition but with very different structures.[4–7] For homogeneous particles, various structures or phases can be in competition with each other depending on size, temperature, preparation method and the possible presence of some environment such as the substrate or coating ligands. The situation becomes even more complicated with heterogeneous nanoparticles such as nanoalloys, due to the additional role played by chemical order or disorder between the various elements within the nanoparticle. This complexity is already manifested in bulk alloys by the phase diagrams that for many elements are not known with high accuracy but require extrapolation based on limited data.

In this article we discuss the specific issue of thermodynamical stability, and more generally the role of temperature on the stable structures and phases of bimetallic nanoalloys. Kinetic stability can of course prevail on thermal stability, and many avenues of current research in nanoscience specifically aim at producing particles that are pretty far away from their most stable shape but whose structure remains as specifically tailored under long enough time scales to enable valuable use. Although kinetic stability may be sufficient for applications, it is important to characterize the equilibrium thermodynamics of nanoalloys and their sensitivity to changes in external conditions. Thermal stability is all the more essential as the nanoparticles are used over extended time periods, as in the fields of nanomedicine or information storage based on mag-

[a] Laboratoire Interdisciplinaire de Physique, Rue de La Piscine, Campus Saint Martin d'Hres, 38000 Grenoble, France, E-mail: florent.calvo@ujf-grenoble.fr

netic materials.

Archetypal structures or phases of bimetallic nanoalloys at finite temperature have been depicted in Fig. 1 mostly for future reference in the rest of the article. Those phases differ in their chemical order, and do not include the additional variety of geometric shapes that can be adopted by generic metallic nanoparticles.[5,7] Among those structures, several phase
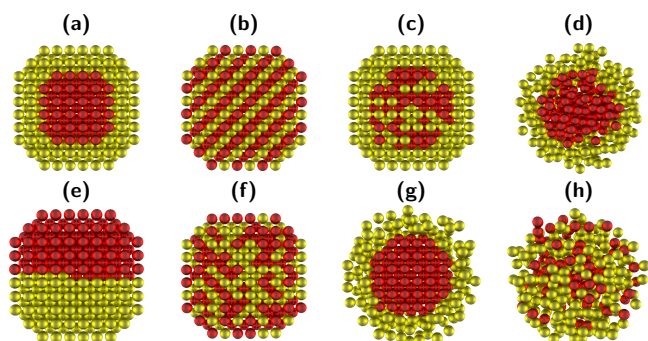

Fig. 1 (Color online) Archetypal patterns exhibited by bimetallic nanoalloys at various temperatures. (a) Solid core/shell; (b) Ordered alloy; (c) Alloyed core/pure shell; (d) Liquid core/shell; (e) Janus-like; (f) Random alloy; (g) Solid core/liquid shell; (h) Alloyed liquid.

separated solid configurations can be distinguished either as core/shell (a) or fully segregated and so-called Janus-like (e), as well as some fully mixed, but still solid configurations either as an ordered (b) or random (f) alloy. As in bulk alloys, additional intermediate situations can occur such as a core alloy surrounded by a pure shell (c). Those five configurations mostly differ from each other by the nature of chemical order or disorder within a given solid structure. As temperature is increased, a part of the system may melt, most likely its surface first as in case (g). Complete melting may be associated with mixing (h) or not (d). At equilibrium, the thermodynamics of nanoalloys aims to determine which of such typical phases are most stable as a function of size, composition and temperature as well as other possible external factors due to a possible environment.

One widespread approach to the thermodynamics of nanoalloys considers a top-down reduction of macroscopic concepts, trying to incorporate finite-size effects as corrections to presumably dominant bulk effects. This point of view is natural for nanoparticles that are large enough and in the so-called scalable regime, and provides a general framework to construct or interpret entire phase diagrams.[8] In very small systems of a few nanometers, each atom may count and the macroscopic perspective could no longer hold. For instance, the empirical Hume-Rothery dissolution rules[9] would not be able to explain why iron and silver mix in clusters despite being immiscible in the bulk.[10] This complementary bottom-up

point of view is sometimes necessary in order to capture new qualitative behaviors or finer effects lying beyond mere surface corrections. Both points of view have their own merit and will be discussed below in more details. However, it is instructive at this stage to illustrate the complexity of nanoalloys thermodynamics by showing some cases of non trivial thermally-induced transformations in nanoalloys that cannot be simply explained based on the knowledge of bulk properties only. We have done so in Fig. 2 by selecting two such examples. In their experimental work,[11] Wen and Krishnan
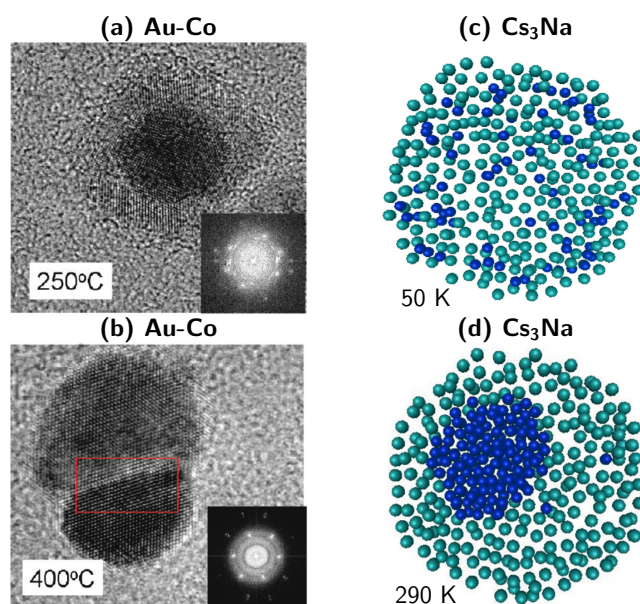

Fig. 2 (Color online) Two examples of thermally-induced morphological changes in nanoalloys. Extrusion of a gold core from a core-shell Au-Co nanoparticle (a) leading to a Janus-type nanoparticle (b). [Adapted with permission from T. Wen and K. Krishnan, Thermal stability and morphological transformations of $Au_{core}-Co_{shell}$ nanocrucibles, *J. Phys. Chem. C*, **114**, 14838-14842. Copyright (2010) American Chemical Society.] (c) and (d) Core-shell segregation in Cs_3Na nanoalloys found in molecular dynamics simulations. [Adapted from M. H. Ghatee and K. Shekoohi, Structures, thermal stability, and melting behaviors of bimetallic Cs-Na clusters studied via molecular dynamics simulations, *Fluid Phase Eq.*, **355**, 114-122, copyright (2013) with permission from Elsevier.]

synthesized by wet chemistry some gold-cobalt nanoalloys in a core/shell configuration [Fig. 2(a)], as inferred from transmission electron micrograph (TEM) analyses. Upon annealing at 400°C the shape of those nanoparticles transformed into that of a peanut, keeping a complete phase separation but minimizing the strain between the two metals [Fig. 2(b)]. Those particles lie in the immiscibility composition range, hence the effect is a pure consequence of the nanoscale and the presence of a surrounding shell of ligands. In the computational

work of Ghatee and Shekoohi, [12] alkali Cs_3Na nanoparticles of about 2700 total atoms were found to be highly miscible in the low temperature solid [Fig. 2(c)], in contrast with the bulk diagram at this composition, but near room temperature a phase separated liquid was found [Fig. 2(d)]. Similar temperature-induced demixing transformations have been predicted in the Ni-Al and Cu-Au systems at the nanoscale. [13,14]

In dealing with nanoalloys at thermal equilibrium, one ultimate goal could be the determination of the three-dimensional phase diagram as a triple function of composition, temperature and size. As in monatomic particles there is no reason to believe that such diagrams would look smooth at small sizes, [8] and more likely be meaningful in broad size ranges. Towards this ambitious goal it would be necessary to characterize the various transitions involving the different metals, their miscibility and resistance to temperature changes, given that the geometric structure itself may depend on siz. [15] and temperature. [16] More modest objectives can be laid out on the way to the construction of entire diagrams. Order-disorder transitions primarily involve the chemical degrees of freedom, but can be rather complex in nanoparticles. The melting transition, which also has peculiarities that cannot be all derived from bulk considerations, is another situation deserving a treatment for itself.

In the following sections we have chosen to describe the phenomenology and diversity of nanoalloys thermodynamics, focusing on the results rather than on details of experimental or theoretical methods. Section 2 presents some general considerations about finite-size thermodynamics that are relevant to pure and multicomponent systems, Sec. 3 providing some basic introduction to common approaches from the two complementary perspectives of the (scalable) bulk and (non-scalable) molecular regimes. Section 4 addresses the case of segregation patterns, which is the simplest example where size, composition and temperature all influence the stable alloy. The order-disorder transition discussed in Sec. 5 is another specific example driven by chemical degrees of freedom rather than atomic variables. Melting in alloys is much more complex than in homogeneous metals, and remains so in nanoalloys. Some discussion is devoted to the melting process in Sec. 6. Once those specialized topics are covered, we are able to describe some phase diagrams in Sec. 7. Finally, the article concludes on some generic considerations about the role of kinetics and thermodynamics in nanoalloys away from equilibrium.

Before proceeding, it should be mentioned that this perspective by no means pretends to be exhaustive, but only serves the purpose of illustrating the diversity and complexity of thermodynamics in nanoalloys. We have chosen not to discuss indirect effects of temperature, which would of course impact physical or chemical properties and even drive entire effects such as Ostwald ripening, [17] but instead to focus on the equi-

librium state of the nanoalloys themselves. In view of its limited size, this perspective only cites a selection of the increasingly vast amount of research groups who are currently active in the field, perhaps biased toward theory and simulation. Any omission is regretted in advance but unintentional.

2 Finite-size thermodynamics

The concepts of phases and phase transitions strictly refer to the macroscopic limit, and one may first question whether the terminology is appropriate in finite-size systems. In the context of condensed phases and metallic systems with very low vapor pressures, the solid and liquid states would seem reasonably easy to define from the atomic perspective, the particles being either localized around their equilibrium positions or alternatively free to move and diffuse in a limited volume, and for both phases irrespectively of the possible presence of multiple elements. However, these intuitive definitions hide some subtle difficulties specific to the finite nature of nanoparticles, and it is necessary to review some of the characterizing aspects of phase transitions, or more appropriately phase changes, in small systems. [18] Those concepts are relevant to conventional, first-order transitions such as order-disorder or solid-liquid transitions that are also present in nanoalloys.

Macroscopic and finite-size thermodynamics differ on several ways. From a fundamental point of view, the statistical ensembles become non equivalent in a finite system, [22] and more generally for systems whose dimensions become comparable to the range of the interaction such as self-gravitating clusters. Although of limited practical importance, this nonequivalence has significant consequences on the theoretical treatments of equilibrium thermodynamics and even counter-intuitive manifestations with the possible presence of negative (microcanonical) heat capacities. [19] Other fundamental differences between macroscopic and finite-size thermodynamics have been suggested, such as the possible violation of the second law over limited time scales. [20]

With the aforementioned limitations in mind, it is conceptually easier to use the statistical formulation of thermodynamics, which is always valid and provides a connection between the potential energy surface defined at the molecular level and the global thermal properties such as enthalpy or heat capacity through the partition function Z. The occurence of phase transitions as a thermodynamic parameter is varied is a manifestation of a singularity in Z, or an accumulation of zeros in the complex plane according to the Yang-Lee theorem. [21] Such singularities cannot occur in finite systems, because the partition function is always analytic for all possible values of the thermodynamic parameter (and for a realistic and well-behaved potential energy surface).

The primary manifestation of a first-order phase transition in a macroscopic system is a sudden jump in the caloric curve

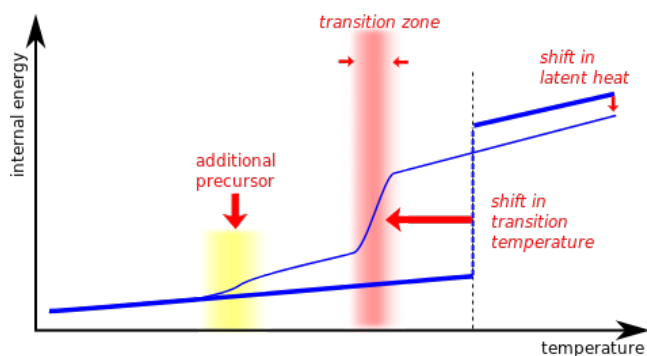known as the latent heat, as sketched in Fig. 3. Several ex-

Fig. 3 (Color online) Schematic caloric curve of a nanoparticle undergoing a first-order finite size phase transition. Only the non-ideal part of the internal energy is shown as a function of temperature. The macroscopic limit is depicted as the two thick lines separated by the vertical dashed line marking the transition. The various red arrows illustrate the main changes occuring in finite size systems.

perimental and theoretical studies have identified three main consequences of a decrease in the system size on its caloric curve:

(i) The transition remains but is shifted, usually to lower temperature, as a result of surface atoms being less co-ordinated and less bound than interior atoms;

(ii) The transition is no longer sharp but becomes smooth and takes place over a finite temperature range, as the consequence of the analyticity of all statistical functions and their fluctuations;

(iii) The latent heat associated with the transition is also lower than in the bulk limit.

The first of these phenomenological observations was predicted long ago by Pawlow[24] in the case of the melting transition, who realized the importance of surface energies in the modification of bulk properties. By combining the Gibbs-Thomson equation for phase equilibrium with the Laplace equation for the surface pressure, several authors have proposed capillary models for the transition in mescoscopic particles that essentially relate the transition temperature $T(R)$ for a particle with radius R to the bulk transition temperature $T(\infty)$ as[18]

$$T(R) - T(\infty) \approx -\frac{\alpha}{R}, \qquad (1)$$

where α is a constant parameter that depends on bulk properties only such as the surface tensions of the various interfaces, the latent heat of the transition in the bulk limit and

the densities of the two phases. The scaling in $1/R$ is characteristic of a 3D spherical particle, and expresses the importance of surface energies (which scale as $E_s \sim N^{2/3}$ with the number of constituents) relative to bulk energies (which scale as $E_b \sim N$), the total energy being approximated as $E_b + E_s \sim N(1 + \delta N^{-1/3}) = N(1 + \delta/R)$.

The $1/R$ law of variation is central to most macroscopic approaches to nanoalloys that attempt to capture the size variations of phase boundaries, as implemented e.g. in the CAL-PHAD software[40] but also in independent models such as those developed by Wautelet and coworkers.[23] In the context of melting, it was first clearly experimentally demonstrated by Buffat and Borel for deposited gold nanoparticles.[25] Despite being generally observed for metals and also rare gases,[26] it should be noted that the $1/R$ depression low is not fully universal and does not seem to hold for semiconducting particles where the shift appears to be linear in $1/R^2$.[27]

The second quantitative difference between finite-size and bulk thermodynamics is the smoothening (or broadening) of the phase transition from a well-defined temperature to a broader range. This effect originates from the fluctuations in thermodynamical quantities which scale as $1/\sqrt{N}$ with increasing size and thus become significant for low values of N. Imry[29] has developed a simple but consistent theory of fluctuations for finite size phase transitions explaining this effect, but we follow the alternative, perhaps simpler model of Berry and coworkers to the same illustrating purpose.[28] Let us assume a system with N atoms in equilibrium between the low-temperature phase A and a high-temperature phase B, with corresponding chemical potentials μ_A and μ_B that depend only weakly on temperature. At temperature T the ratio between the concentrations of phases B and A equals $K = [B]/[A] = \exp[-N(\mu_B - \mu_A)/RT]$, where R is the perfect gas constant. For a bulk system, $K = 1$ exactly at the transition temperature $T = T^*$, $K = 0$ at $T < T^*$ and $K = +\infty$ at $T > T^*$. However, for a finite-size system $\mu_B - \mu_A$ remains nonzero but the ratio K is only exponentially vanishing, it thus takes finite values in the vicinity of T^*.

The same reasoning lead Imry to establish a simple law for the uncertainty $\Delta T(R)$ on the transition due to fluctuations, which he found to scale as $1/N$ or, in the case of spherical particle, as[29]

$$\Delta T(R) \approx \frac{\beta}{R^3}. \qquad (2)$$

The fluctuating state predicted by this theory corresponds to the entire system being entirely in either phase but with a finite probability, but does not refer to equilibrium between the two phases within the same system.

In nanoalloys, reduction in the transition temperature and increase in the statistical fluctuations as particle size decreases may also produce an interesting contradictory phenomenon known as the depletion effect.[30] Briefly, this effect arises in

systems for which the formation of a new phase would require a certain amount of matter of a given species to nucleate. If the system is too small, this critical amount would not be reached and phase transformation would be suppressed. Similarly, the decrease in the transition temperature predicted by capillary models necessarily has some limitations when the depression becomes of the order of the bulk transition temperature itself, at which stage a more atomistic approach should be adopted.

The third regular manifestation of finite-size effects on first-order phase transitions is the decrease in the latent heat L associated with the transition. Capillary models involving an equilibrium between the two phases in a core-shell fashion have also been developed in this respect[31] and shown to produce a depression in L that scales as $1/R$, following the contribution of surface energies to the global binding. So far those predictions have been validated against nanocalorimetric measurements in the case of the melting transition in deposited tin particles.[31]

The generic shifting and broadening of the caloric curves in individual systems should be considered as the dominant finite-size effect in nanoparticles decreasing from the bulk limit. As the size of nanoparticles becomes very small, the non-scalable regime is reached and additional features in the caloric curves can take place. Those features originate from physical or chemical elements that cannot be considered simply as global surface effects, but could depend on finer details such as defects that promote surface melting,[32] or competing structures leading to entropy-driven transitions.[16,33] Such precursors to the main transition have been experimentally reported in the case of pure[34] and doped[35] aluminum clusters, but are generally not systematic. From the theoretical point of view they are difficult to predict from pure macroscopic considerations, but are more amenable to detection and interpretation based on computer simulations.

The detailed electronic structure may also become increasingly important in small clusters, either indirectly via the stable structures produced or more directly through changes in chemical bonding. One remarkable consequence of the influence of chemical bonding on nontrivial variations in transition temperatures is for instance the unexpectedly high melting point reported in gallium clusters,[36] and since interpreted as due to the partially covalent character of bonding in such small systems.

3 Experimental and computational approaches to nanoalloys thermodynamics

We wish now to briefly describe some of the generic methods for addressing the thermodynamics of nanoalloys. From the experimental point of view, nanocalorimetry explores the response to a temperature change on various physical or chem-

ical properties. For particles deposited on a substrate, diffraction techniques or high-resolution microscopy provide direct insight into the crystalline and chemical ordering within the particle. Strong thermal changes such as melting can also be probed using differential scanning calorimetry (DSC). If the particles have narrow distributions in size and composition, global information about the phase diagram can thus be evaluated, and in-situ TEM measurements can even be used to monitor phase changes in individual nanoparticles.[37]

For particles produced in the gas phase, the internal energy can be estimated based on the propensity of nanoparticles for dissociation, leading to a fairly complete determination of entire caloric curves.[19] Owing to mass spectrometry techniques, measurements in the gas phase can be carried on well-defined sizes and compositions, and sometimes even on individual (trapped) particles.[38]

Computational methods to address the thermodynamics of nanoalloys mainly fall into two main categories. Approaches based on classical thermodynamics attempt to combine macroscopic models developed for bulk alloys with finite-size corrections for surface energies, given spherical particles for simplicity. Typically the Gibbs free energy of a spherical alloyed particle with elements A and B mixed together would be expressed by a relation of the type

$$\begin{aligned} G(N) &= x_A[N\mu_A + \sigma_A N^{2/3}] + x_B[N\mu_B + \sigma_B N^{2/3}], \\ &+ RT[x_A \ln x_A + x_B \ln x_B] \end{aligned} \tag{3}$$

where x_A, μ_A and σ_A denote the molar fraction, chemical potential, and surface energy of element A, respectively. The expression for the free energy distinctly shows the different contributions of the surface ($N^{2/3}$ terms) and of configurational mixing (entropy terms in $x \ln x$ that are characteristic of a solid solution). Such a model assumes that the interactions between atoms are the same in the alloy as in the homogeneous compounds and that there is no segregation or surface enrichment. More refined approaches require additional terms and parameters such as interaction energies as a function of the molar fractions or more realistic composition dependencies of the surface tension, e.g. from the Butler equation,[39] or in the case of phase separated systems estimates of the interfacial energies and strain energies for the solids. Such global thermodynamical models are now being implemented in the so-called CALPHAD method, originally designed to supply quantitative thermodynamical data for industrial purposes,[40] and which is gaining some momentum in the context of nanoscience even from the fundamental perspective.[41] Some applications of the classical thermodynamical approach to nanoalloys will be given below.

The second major theoretical approach to nanoalloys thermodynamics relies on computer simulation. It is complementary to the classical method in the sense that it is provides details at the atomic level and does not employ macroscopic

assumptions, however it requires some knowledge of the interactions and, at finite temperature, some statistical sampling of the thermal distributions. Unfortunately, the interactions obtained from first-principles (generally density-functional theory - DFT) are extremely computer intensive and one rather widespread approach uses semi-empirical analytical potentials, typically parameterized on bulk properties but sometimes refined using nanoclusters data. Thermodynamical equilibrium is usually simulated by molecular dynamics (MD) or Monte Carlo (MC) methods, from which many properties and order parameters can be calculated whose variations are to be related to changes in the thermodynamical observables.

The atomistic simulation approach is particularly useful to tackle the melting transition, which lacks a general ab initio theory even in the bulk case. Other specific transitions, such as those involving chemical order but not affected by geometrical changes, can be simulated using even simpler lattice models possibly derived from more realistic off-lattice methods. In general, for the results to be meaningful of a true thermodynamical equilibrium care should be taken to explore broad regions of configuration space. Computational tricks such as replica exchange [42,43] or multicanonical sampling [44] are thus generally recommended to improve ergodicity in the MD or MC simulations.

4   Segregation patterns

One issue with multicomponent particles that is of central importance in surface science and in particular catalysis is the determination of the distributions of the various components within the particle. This situation is mostly interesting for alloys that readily mix in the bulk, but that could exhibit some separation once at the nanoscale. Such segregation patterns are experimentally accessed through microscopy but also, more sensitively, by probing the environment of individual atoms through their electronic structure using e.g. extended X-ray absorption fine structure (EXAFS) or X-ray photoelectron (XPS) spectroscopies. [3]

The factors influencing segregation are primarily those responsible for the main features of the bulk phase diagram, namely the relative magnitudes of the interactions (including charge transfer due to electronegativity differences) and the possible mismatch between atomic sizes. At the nanoscale additional factors come into play, starting with the relative surface energies and the possibility to coat the particles with surfactant molecules, with different responses to the different local environments. At finite temperature, small energy differences separating mixed from segregated patterns could be overcome by thermal excitations, hence it can be important to consider this parameter as well.

The gold-palladium system is a good example of a miscible alloy in the bulk, but whose free surface has been recently

suggested to be enriched in gold, [45] in contradiction with earlier experiments. [46] Atanasov and Hou [47] conducted a detailed Monte Carlo investigation of the segregation patterns in Au-Pd nanoalloys containing about 1000 atoms at finite temperature ($T = 100$ K), using an atomistic potential energy surface in the so-called semi grand-canonical ensemble (SGC Monte Carlo or SGCMC). In the SGC ensemble, the total number of atoms and temperature are fixed, as well as the chemical potential difference $\Delta\mu = \mu_A - \mu_B$ between the two elements A and B, leaving the composition allowed to vary as a function of temperature and particle shape. The physical significance of the SGC ensemble is not straightforward, but fixing the chemical potential difference should be understood as the presence of reservoirs supplying the necessary number of atoms of both types under the form of atomic vapors at specified partial pressures.

The segregation isotherms or relative concentration in palladium were determined for the various shells of a Wulff particle (truncated octahedron of 1289 total atoms), namely the 459 core atoms, the 482 outermost atoms, and the 348 intermediate or subsurface atoms, as a function of $\Delta\mu = \mu_{Pd} - \mu_{Au}$, and reproduced in Fig. 4(a). As the chemical potential difference increases, the nanoparticle progressively transforms from pure gold to pure palladium. The intermediate regime displays plateaus in the segregation isotherms, and summing the different contribution of the subshells clearly shows that the transition is not sharp (as it would be in the bulk), the propensity of each atom to transmute into Pd depending on its local environment. The stability plateaus are rather prominent for this highly symmetric particle and associated with the filling of shells or subshells. As clearly seen from the calculations the core and subsurface parts of the particle transmute into palladium much earlier than the surface atoms as the chemical potential is tuned toward Pd. The surface enrichment in gold predicted by the calculations, illustrated in Fig. 4(a) on three stable configurations obtained for different values of $\Delta\mu$, is thus consistent with the more recent experiments. [45]

In contrast to Au-Pd, the copper-silver system is generally immiscible in the bulk and expected to form phase separated nanoalloys with silver at the surface owing to its lower surface energy. This has been verified in experiments, [48] but some detailed computer simulations have revealed some unexpected mechanisms associated with the superficial segregation in the copper-dominated regime. Using atomistic models and a SGCMC computational protocol similar to the one of Atanasov and Hou, Delfour and coworkers [49] first predicted a clear ordering in the preferential segregation of silver at the surface sites, starting with vertices, then edges, (001) and finally (111) sites. The corresponding isotherms, represented in Fig. 4(b), additionally exhibit smooth but concomitant jumps near $\Delta\mu = \mu_{Ag} - \mu_{Cu} = 0.39$ eV that are indicative of a transition to a differently segregated phase with more silver at
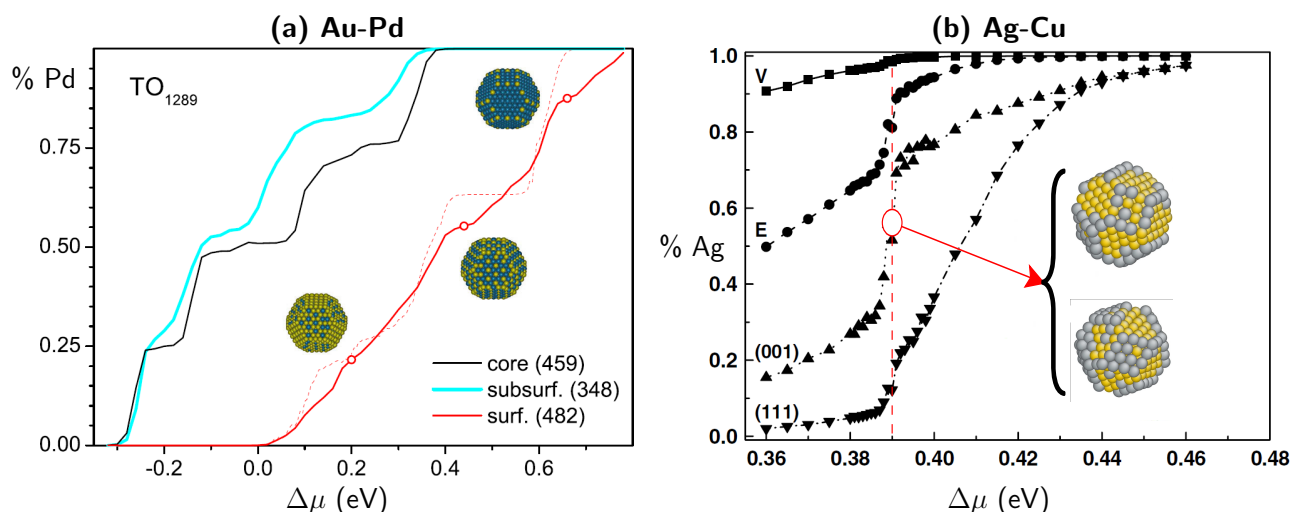
Fig. 4 (Color online) Examples of segregation patterns obtained from Monte Carlo simulations of bimetallic nanoalloys with truncated octahedral shape, and showing stability plateaus associated with shell filling. (a) 1289-atom Au-Pd cluster at 100 K, with the specific contributions of core, surface, and subsurface atoms. Three particularly stable configurations are highlighted. [Adapted from I. Atanasov and M. Hou, Equilibrium ordering properties of Au-Pd alloys and nanoalloys, *Surf. Sci.*, **603**, 2639-2651, Copyright (2009) with permission from Elsevier.] (b) Silver fraction in 405-atom Cu-Ag nanoalloy at 300 K, and equilibrium phase predicted at $\Delta\mu = 0.39$ eV involving a square shape at low Ag concentration with a diamond shape at high Ag concentration. [Adapted from L. Delfour, J. Creuze, and B. Legrand, Exotic behavior of the outer shell of bimetallic nanoalloys, *Phys. Rev. Lett.*, **103**, 205701, Copyright (2009) by the Americal Physical Society.]

the surface. The fluctuations turn out to be maximum at this value of the chemical potential difference but quite insightful as well. Inspecting the pseudo-time series and statistics of the Monte Carlo trajectory reveals the presence of two phases that coexist with each other, differing mostly in their (001) faces not only in the amount of filling, but also in some possible distortion in the case of large silver filling, as depicted in Fig. 4(b). The presence of significant lattice distortions in the silver-filled case is explained by the large lattice mismatch between the two elements. This equilibrium between two chemically but also geometrically different shapes is a strict finite-size effect that can be described by the fluctuations theory discussed above. In large Ag-Cu nanoparticles, it should thus also be present but in a vanishingly narrow range of chemical potential difference.

Other exotic segregation patterns have been suggested in computations, e.g. in the case of Pd-Pt nanoalloys. Although the Pd-Pt system forms a solid solution in the bulk, experiments[50,51] have reported that the surface of nanoalloys is Pd-enriched. DFT calculations[52] have nevertheless found that Pt atoms could segregate to the center of (111) outer facets in order to minimize the global strain within the nanoparticle, the interior shells exhibitting reverse patterns in which Pd and Pt alternate with each other between shells. This alternation confirms earlier theoretical[53] and experimental[54] suggestions that the most stable structure of large Pd-Pt nanoparticles could indeed be of the multishell or 'onion-ring' type.

Because segregation patterns at finite temperature cannot be investigated with an explicit account of electronic structure simultaneously with statistical sampling for particles containing a reasonable number of atoms, several models have been developed to exploit the DFT data into simplified, lattice-based descriptions nanoalloys. In the coordination-dependent bond-energy variation model of Polak and Rubinovich,[55] the energy at each site of a given lattice depends on the environment through explicit functions of the coordination that are parametrized on electronic structure reference data. For this Ising-type model, the stable phase at finite temperature can be computed numerically by minimizing a free energy over all possible chemical configurations of the nanoparticle, written using partition functions expanded in atomic concentrations beyond the mean-field approximation by incorporating local ordering effects.[56]

A related strategy has been adopted by Johnson and coworkers[57] who derived a cluster expansion for the energy of an individual atom on a specific lattice as a function of its local environment,[58] using again DFT data to parametrize the coordination-dependent site energies. In contrast with the previous semi-analytical approach of Polak and Rabinovich, Johnson and coworkers sampled the finite-temperature behavior of the nanoalloy by MC simulations. Although this may be not as esthetic, the Monte Carlo approach is perhaps more rigorous because it fully incorporates statistical fluctuations that could be essential in small systems but necessarily absent

when minimizing exactly a free energy functional.

An interesting extension of the cluster expansion method was recently made toward ligand-coated Pd-Rh nanoparticles.[59] Such nanoalloys have been experimentally shown to be enriched in rhodium under oxidizing conditions, while being enriched in palladium under reducing conditions.[60] While this behavior can be qualitatively explained by the stronger interaction of oxygen with rhodium relative to palladium, much more insight can be obtained from dedicated modeling. In their computational study of 55-atom clusters, Wang and coworkers[59] considered the possibility for surface atoms to be bound to external atomic oxygen, in addition to the normal alloying variables. All oxygen atoms were restricted to sit on specific lattice sites, and the model was parametrized further to take into account the adsorption energies of oxygen over various possible sites. The Monte Carlo simulations, partly reproduced in Fig. 5, reveal a marked dependence of oxygen coverage on the segregation of the outermost surface, which becomes increasingly rich in rhodium as oxygen pressure increases. By scaling those results appropriately, good agree-
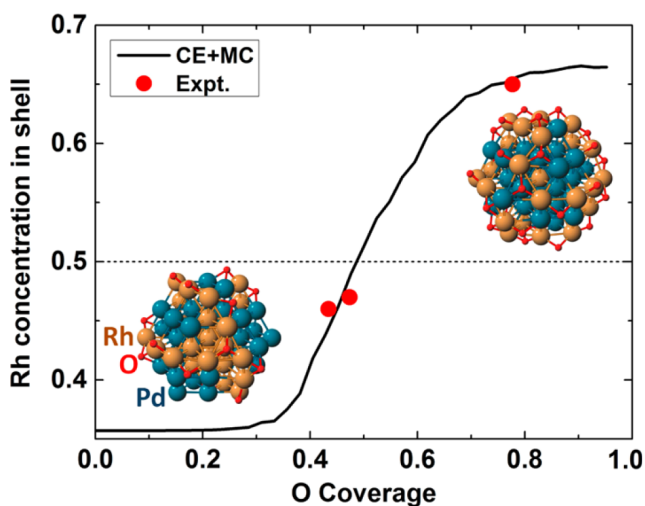

Fig. 5 (Color online) Outer concentration of rhodium in 55-atom Pd-Rh nanoalloys as a function of surrounding oxygen coverage, as obtained from experiment and Monte Carlo simulations based in a cluster expansion of the formation energy. [Reproduced with permission from L.-L. Wang, T. L. Tan and D. J. Johnson, Configurational thermodynamics of alloyed nanoparticles with adsorbates, *Nano Lett.*, **14**, 7077-7084. Copyright (2014) American Chemical Society.]

ment is obtained with experiments carried out on larger (15 nm) particles.[59]

Obviously lattice-based methods are mostly valid for nanoalloys that combine miscible elements without a large size mismatch. Their main advantage is that most of the computational cost resides in the initial parametrization by elec-

tronic structure methods, after which the lattice model is transferable to arbitrary sizes and compositions, possibly through reduction in the number of degrees of freedom based on symmetry. However, those methods would not be accurate if important relaxations take place, as identified in Fig. 4(b) for Cu-Ag particles. The fully atomistic approach is then a method of choice, although care should be taken that its parameters are also transferable from the bulk to surfaces and nanoparticles.

5 Order-disorder transition

Many metals readily form ordered alloys [or intermetallic compounds as depicted in Fig. 1(b)] when combined together at selected compositions and sufficiently low temperature. Intermetallics acquire their mechanical or electronic properties from the specific crystalline order they adopt, usually for the best although in some cases degradation is found. The control of chemical order in intermetallics is of particular importance for magnetism, magnetic moments being generally strongly attenuated in the solid solution phase [Fig. 1(f)]. Metal clusters and nanoparticles have been experimentally shown to possess enhanced magnetic moments relative to the bulk limit.[61] The potential of such particles, once deposited and assembled in a stable way in high-density information storage devices has naturally motivated significant work in the context of nanoalloys. Bimetallic alloy nanoparticles based on cobalt (Co-Pt, Co-Rh) and iron (Fe-Pt, Fe-Pd) have notably been shown to possess magnetocrystalline anisotropy constants much larger than some of the current alloys used in magnetic devices such as cobalt-chromium.[62] However, in absence of chemical ordering the nanoparticles become superparamagnetic, which renders them useless at moderate temperatures due to the impossibility of preserving magnetization under thermal fluctuations. It is thus important that the nanoparticles are in the ordered alloy state for practical applications.

The order-disorder transition in bulk intermetallics into the high-temperature phase is of the first-order type, the low-temperature ordered phase being associated with low energy and entropy but high short- and long-range orders that confer to the magnetic materials their largest coercitivity. In contrast, the high-temperature phase is associated with a higher energy, a very high entropy associated with random alloying [see last term of Eq. (3)], an a loss in both short- and long-range ordering. The order-disorder phase change in alloy nanoparticles provides a first archetypal example of finite-size effects on first-order phase transitions.

Order-disorder transitions in many alloys can be seen as involving only chemical degrees of freedom on a fixed lattice (usually face-centered cubic), thus reducing the problem to the Ising class. This has lead some groups to model the order-disorder transition in bimetallic nanoparticles using lattice-based Monte Carlo simulations, notably for the important Fe-

Pt alloy.[63–65] Those investigations generally confirmed the shifting and broadening of the order-disorder transition as the particle size is decreased from the bulk limit, in agreement with earlier statements. This lowering in the transition temperature is problematic for applications because it means that at a fixed temperature the smaller particles might be chemically disordered and not valuable for magnetic applications.

The order-disorder transition has received particular attention in the case of Co-Pt nanoparticles near equiconcentration. Under such conditions it involves the ordered $L1_0$ phase at low temperature and the random alloy (A1) at high temperatures. Experimental evidence for chemical ordering at low temperature comes from magnetic SQUID measurements[66] but also, more directly, from electron microscopy.[67] We have represented in Fig. 6(a) an electron micrograph obtained for a 3.8-nm diameter CoPt nanoparticle viewed along the (110) axis and generated under appropriate annealing scheme.[67] In the same experiment, a marked dependence of the ordering ability of nanoparticles on their size was observed, particles smaller than 0.5 nm diameter being always chemically disordered. Again, much insight has been brought by Monte Carlo simulations.[67,68] Using an off-lattice model described by a semiempirical potential[69] Mottet and coworkers have simulated the order-disorder transition in CoPt nanoparticles covering the size range $N = 400$–1300 or 2–3 nm diameter.[67,68] The short-range order parameter (SRO) introduced by Cowley[70] to probe the local chemical environment around individual atoms is well suited to monitor the order-disorder transition, and we have represented in Fig. 6(b) the outcome of such simulations for nearly spherical nanoparticles with different sizes and also for an elongated (1.5×4)-nm particle containing about 1500 atoms.[67]

The variations of the SRO parameter clearly demonstrate the decrease in the transition temperature with decreasing size, as well as a significant broadening in the elongated particle. For the latter system, with approximately as many atoms as in the 3-nm diameter nearly spherical particle, the transition temperature is not markedly altered but the broadening is a consequence of the presence of different characteristic dimensions all with their own thermal response. The caloric curves reported for the same systems[68] exhibit clear peaks in the heat capacity that increasingly broaden as the particle size decreases, concomitantly with a decrease in the latent heat of the transition. Together with the depression in the transition temperature, these three manifestations of finite-size effects on a first-order transition are consistent with earlier considerations discusses in Sec. 2.

MC simulations provided further details about the mechanisms of the transition, and notably showed that it is triggered not uniformly but is rather initiated at the surface.[63,65,68,71] In addition, the relatively large tetragonalization ratio of the ordered $L1_0$ phase was found to be essential, lattice descriptions

producing a much broader and unrealistic transition already in the bulk.[68] This importance of anisotropy in the interactions matches the strong influence of particle shape on the broadening of the transition in elongated samples.

The order-disorder transition in CoPt nanoparticles is archetypal of a first-order phase change but is not limited to the 50% concentration. Most stoichiometries forming stable alloys in the phase diagram, e.g. Co_3Pt and $CoPt_3$ in the $L1_2$ phase, are prone to undergoing a transition to the solid solution at high enough temperature. By varying composition in addition to temperature, entire phase diagrams can be constructed (vide infra).

6 Melting

Similarly as the ordered state is a prerequisite for some bimetallic nanoparticles to acquire they magnetic moments, many applications require the particles to be stable in solid form. If the depression in the transition temperature mentioned in Sec. 2 applies to the melting transition, then it is expected that sufficiently small particles might destabilize upon heating even at moderate temperatures, which would clearly impede the ultimate miniaturization in electronic circuitry. The same concerns exist in nanoalloys, and more generally various authors have attempted to characterize the melting transition in multimetallic nanoparticles, both experimentally and theoretically, with a bulk or an atomistic perspective.

The melting behavior of mixed Pb-Bi nanoparticles of diameter 5–40 nm and near the atomic concentration of 51–56% in bismuth has been experimentally investigated by Jesser and coworkers.[72] These authors performed electron microscopy measurements on assemblies of deposited particles, and found for diameters greater than 6 nm a two-stage melting process, with the formation of a liquid layer of finite and approximately constant thickness in equilibrium with a solid core at temperature T_s, corresponding to the so-called solidus or the upper limit of stability of entirely solid system. Upon further heating the core was found to shrink down and eventually melt as well at the temperature T_ℓ, corresponding to the liquidus or lower limit of stability of the entirely liquid phase. Both solidus and liquidus temperatures were determined to approximately vary linearly with inverse particle radius $1/R$, as reproduced in Fig. 7. For particles smaller than 6 nm, the solidus and liquidus temperatures decreased to a common value and the melting process was then found to become single-stage.[72] Chen and coworkers[73] studied melting in silver-lead nanoparticles at the specific eutectic composition where the solidus and liquidus temperatures meet. These authors were able to monitor the composition dependence of the eutectic temperature, and showed that it also scales linearly with inverse nanoparticle diameter. In both works the authors developed thermodynamical models to rationalize their observations.[72,73]
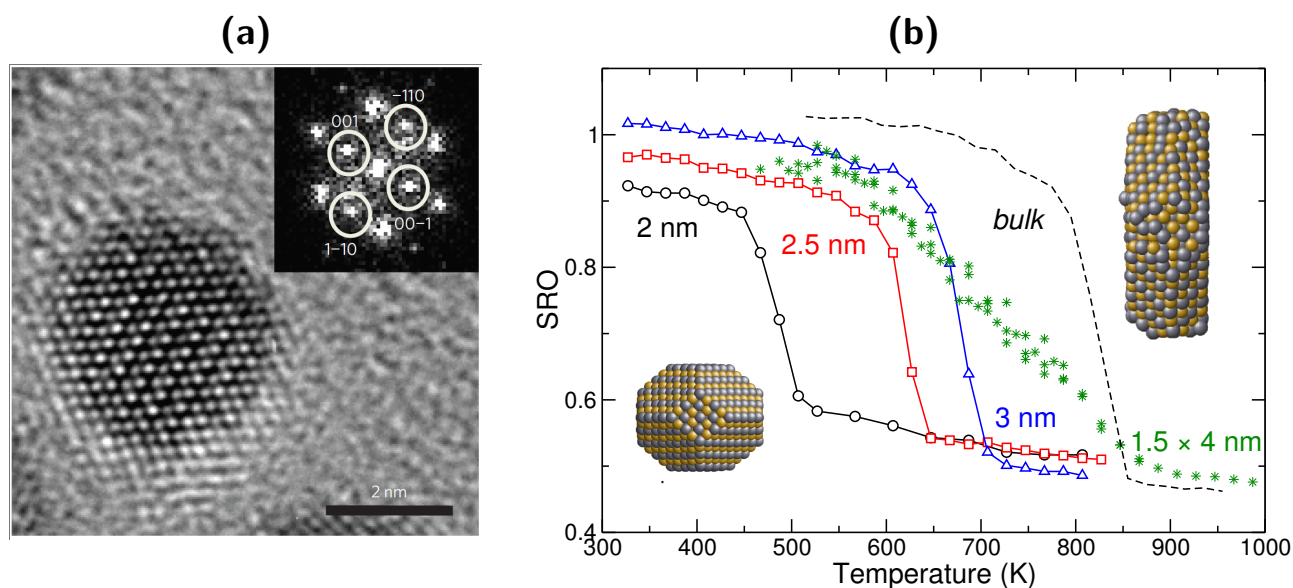
(a)

(b)

Fig. 6 (Color online) Order-disorder transition in CoPt nanoalloys. (a) Experimental high-resolution transmission electron micrograph of a 3.8-nm CoPt particle oriented along the [110] zone axis and showing the $L1_0$ order; (b) Short-range order parameter of simulated CoPt nanoalloys of various sizes (symbols) and a periodic sample (dashed line) as a function of temperature, as obtained from Monte Carlo simulations. The corresponding parameter for an elongated particle with dimensions 1.5×4 nm are superimposed as well. [Adapted with permission from Macmillan Publishers Ltd: D. Alloyeau, C. Ricolleau, C. Mottet, T. Oikawa, C. Langlois, Y. Le Bouar, N. Braidy, and A. Loiseau, Size and shape effects on the order-disorder phase transition in CoPt nanoparticles, *Nature Mat.*, **8**, 940-946, copyright (2009).]

From the molecular perspective, the melting transition has been experimentally addressed in size-selected anionic aluminum clusters doped with a copper impurity by Cao and coworkers.[35] For these very small clusters containing no more than 62 atoms, the impurity was found to play a significant role on the melting temperature with variations of ±10% depending on size. Those intriguing variations could be interpreted based on DFT simulations at finite temperature, which revealed that the atomic relaxation upon substituting aluminum by copper is markedly size-dependent.[35] Such effects of impurities were previously reported in experiments on oxidised sodium clusters,[74] for which the formation of strong ionic bonds leads to a significant increase in the melting temperature.

The role of impurities on nanoparticle melting has been specifically investigated by molecular dynamics simulations by Mottet and coworkers based on semiempirical many-body potentials.[75] Here again the atomistic details provided by such computational approaches were essential to fully interpret the increase in the melting temperature of silver clusters doped with nickel or copper atoms, found to be as large as 50 K in 147-atom clusters. This enhanced thermal stability was interpreted as originating from the stabilization of the (icosahedral) solid phase occuring upon replacement of the central but strained silver atom by a smaller impurity.

Besides providing a rather straightforward and realistic pic-

ture of atomistic mechanisms, the computer simulation approach to melting has additional virtues as connections to thermodynamical concepts can be made through the use of statistical mechanics. In particular, advanced Monte Carlo combined with periodic minimization allow the different roles of structural, chemical, and thermal orders to be disentangled within an energy landscape approach. The various isomers obtained by such procedure can be rationalized in terms of geometries and, among them, the different chemical partitionings of atoms among the structural lattice also known as homotops.[76] The landscape approach to complex system is very fruitful because it provides a transparent interpretation of emergent phenomena, including phase stability and phase transitions, as the result of a change in the equilibrium populations of specific minima or groups of minima.[77] In a first approximation, the order-disorder transition can thus be seen as a switching from a specific homotop at low temperature to a much broader bunch of homotops at a high temperature. Likewise the melting transition can be seen as a switching from a reduced set of minima to a much broader set of structurally disordered and fluctuating minima constitutive of the liquid state.

One application of the landscape approach to the thermodynamics of nanoalloys was proposed in the case of the Pd-Pt system.[53] Although the bulk alloy readily mixes into a solid solution at all compositions, segregation patterns were found in Pd-Pt nanoparticles with a substantial enrichment in palla-
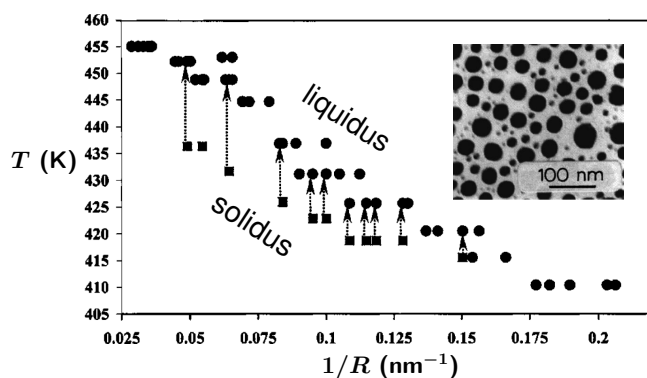
Fig. 7 (Color online) Size-dependence of the solidus (circles) and liquidus (squares) temperatures of Pb-Bi nanoparticles with composition in bismuth varying from 51% to 56% with increasing particle size. The inset shows a bright-field transmission electron micrograph of a sample of deposited particles. [Adapted with permission from W. A. Jesser, R. Z. Schneck, and W. W. Gile, Solid-liquid equilibria in nanoparticles of Pb-Bi alloys, *Phys. Rev. B*, **69**, 144121. Copyright (2004) by the American Physicsl Society.]

dium at the surface.[50,51] Dedicated simulations for icosahedral clusters containing up to a few hundreds of atoms were carried out accross the melting range, and combined with systematic quenching in order to correlate the computed caloric curves to possible changes in the distribution of underlying minima or inherent structures.[53] For all systems the caloric curves showed a well-defined melting change with the expected shifted and broadened features expected for a finite-size phase transition. As anticipated, the inherent structures in the high temperature liquidlike state were found to highly disordered and chemically mixed. However, in the solidlike state quite far below the melting point the equilibrium phase consists of a large variety of homotops of the icosahedral minimum. Only at very low temperature was the lowest-energy structure found as the unique available minimum. These simulations indicate that the solid solution behavior requires thermal energy to become the most stable, and that some order-disorder transition precedes melting even though it is not associated with any apparent precursor in the caloric curve.[53] As the nanoparticle enlarges, it becomes increasingly easy to thermally activate chemical disorder, and the bulk behavior of a fully miscible solid solution is recovered. This phenomenon is actually similar to the emergence of metallicity in metal clusters, where the discrete energy levels characteristic of finite-size systems progressively fill up to form continuous conduction bands in bulk metals.[78]

Using similar methods, the melting transition has been computationally explored in a variety of silver-based nanoalloys combined with gold, platinum, or nickel to a silver ratio of 3:1 and for a total number of atoms in the 55–309 range.[79] These

simulations were carried out to better understand optical absorption spectroscopy measurements[80] that resisted interpretation based on simple alloy or phase separated models. The three systems exhibit very different bulk phase diagrams,[81] Ag-Au being fully miscible as a solid solution, Ag-Ni being fully immiscible, and Ag-Pt having several stable ordered alloy phases. These MC simulations also employed analytical many-body potentials fitted to reproduce bulk properties, and in addition to the pure thermodynamic properties (caloric curve) several dedicated parameters were evaluated in order to analyse the results. The variations with temperature of the heat capacities obtained for the different nanoalloys are reproduced in Fig. 8(a). The surface segregation patterns were determined from the propensity of the outermost atoms to be of the silver type based on local coordination. The variations of this probability with increasing temperature are shown in Fig. 8(b) for the three alloys at total size 309. Radial distribution functions (RDF) were calculated below and above the melting point, separating the contributions from the different atom types. The RDF obtained for Ag-Au and Ag-Pt clusters at size 309 and near room temperature are depicted in Fig. 8(c). A third global property that turned out to be insightful for the Ag-Ni nanoalloys is the global shape and deformation of the nanoparticle. Fig. 8(d) thus displays the temperature variations of the thermally averaged principal momenta of inertia for the 309-atom Ag-Ni nanoparticle. For the three alloys, the heat capacities display increasingly narrow peaks indicative of phase changes rounded by size effects. Clear precursors are systematically found in the smaller 55-atom alloy clusters, but also in the 309-atom Ag-Ni system.

The Ag-Au clusters are essentially mixed in the entire temperature range, no strong surface segregation being found at finite temperature. A slight surface enrichment in silver is generally found but decreases as temperature is increased near the melting point. The radial distribution function confirms the solid solution behavior for these clusters. Ag-Pt nanoalloys are core-shell phase separated at low temperature with silver outside, in agreement with the lower surface energy of this metal. Above the melting temperature of near 700 K, mixing becomes increasingly favored through the entire liquid particle. As shown by the radial distribution functions, an interesting intermediate is found at lower temperatures corresponding to the solid state, with distinct mixing in the core but still a pure silver shell [see Fig. 1(c)]. As the emergence of the solid solution in the Ag-Au or Pd-Pt nanoscale systems, this intermediate phase of an alloy core surrounded by a pure shell occurs without any latent heat. This coexistence of an alloy with a pure phase is consistent with the corresponding region of the bulk phase diagram at the 75% silver composition.[81] Those results incidentally explain why the optical measurements of Cottancin *et al.*[80] could not be explained by the phase separated or fully alloyed limiting models.
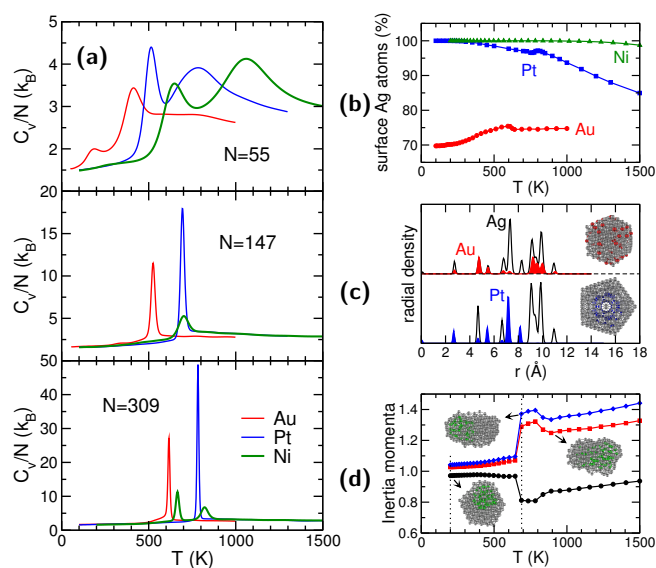
Fig. 8 (Color online) Phase changes in $(Ag_xM_{1-x})_N$ nanoalloys with $x = 0.25$ and $N = 55$, 147 and 309, for $M =$ Au, Pt and Ni, as obtained from Monte Carlo simulations in the canonical ensemble. (a) Heat capacities; (b) Fraction of silver atoms at the surface for $N = 309$ as a function of temperature; (c) Radial distribution functions at 300 K in Au-Ag and Au-Pt nanoalloys for $N = 309$; (c) Averaged and normalised inertia momenta in the Ag-Ni nanoalloy for $N = 309$ as a function of temperature. [Adapted with permission from F. Calvo, E. Cottancin, and M. Broyer, Segregation, core alloying, and shape transitions in bimetallic nanoclusters: Monte Carlo simulations, *Phys. Rev. B*, **77**, 121406(R). Copyright (2008) by the American Physical Society.]

Finally, the low-temperature structure of Ag-Ni nanoparticles is found as a distorted, core-shell phase separated configuration with the core being off-centered, giving the particle a Janus-like character intermediate between the structures depicted in Figs. 1(a) and (e). This anisotropic distribution of the core atoms can be rationalized as a favorable configuration that minimizes both the strain and the energy in the phase separated system, smaller impurities sitting preferentially at the center while face-to-face segregation is expected in very large systems.[82] As temperature is raised, Fig. 8(d) shows that the silver shell melts first, with a strong prolate deformation of the entire nanoparticle that is concomitant with an intense peak in the heat capacity near 600 K. Such deformed nanoalloys have indeed been observed by electron microscopy on similar silver-copper particles.[83] Finally, at even higher temperatures $T > 800$ K a second peak in the heat capacity is associated with the melting of the nickel core itself, with some minor but visible mixing. Such a two-stage melting process has recently been confirmed by molecular dynamics simulations performed by Oderji and coworkers,[84] who found notable differences in the general melting mechanisms

of Ag-M nanoalloys (M=Cu, Ni, Co) depending on the structural arrangements of the outer silver shell, and by Palagin and Doye[85] who searched for possible thermally stable magnetic bimetallic clusters.

Among the increasingly vast literature on computer simulations of nanoalloys melting, a few efforts are worth mentioning further. Although scarce in comparison with semiempirical approaches, first-principle modelings with an explicit account for electronic structure have been achieved by Aguado and coworkers, notably for aluminum-doped clusters[35] but also mixed alkali clusters.[86] Likewise Ojha *et al.* have evaluated the influence of an aluminum impurity on the melting of gallium clusters,[87] which in pure form exhibit higher-than-bulk melting temperature due to covalent contributions to bonding.[36]

The first-principles approach in undoubtly more realistic, but also much more demanding than simulations based on explicit potentials. Melting in nanoalloys in the range of tens to several thousands of atoms has been studied in the case of core-shell bimetallic particles of the Pt-Au,[88,89] Au-Cu,[90] or Co-Au[91] types, where the distinct behaviors of the two metals and their interplay were conveniently scrutinized by following appropriate indices of their atomic mobility such as the diffusion constant or the relative bond length fluctuation. Differences in the melting mechanisms were notably found depending on the size of the core, two-phase melting requiring a core that is neither too small nor too large.[89] Melting of alloyed clusters has also been simulated by molecular dynamics, e.g. by Chen and Johnston[92] who found strong finite-size effects in equiatomic Ag-Au clusters containing between 24 and 140 pairs ot atoms and $(AgAu)_{44}$ as a possible magic number with exceptional stability.

In addition to these studies on isolated particles, some authors have attempted to incorporate the possible effects of the environment. Huang and coworkers[93] and Sankaranarayanan and coworkers[94] have for instance used molecular dynamics simulations to study melting and segregation in nanoalloys deposited on graphite. The substrate was found to delay the melting process quite significantly to higher temperatures and to alter its mechanisms, the liquid nucleating from the free surface rather than the surface in contact with carbon. Another interesting situation is that of nanoparticles embedded in solid matrices. DSC experiments conducted on indium particles inserted in amorphous[95] or crystalline[96] aluminum matrices have produce contrasted variations of the melting point with decreasing size. The strong role of the interface between the two materials was also found in experiments on lead nanoparticles, also in aluminum matrices but with particles prepared using different mechanical methods.[97] One observation of this work, which has been reported in other experiments on silver[98] and copper[99] in different matrices, is the possibility of superheating the embedded particles, that is keeping them

solid even above their (bulk) melting point. Superheating is a direct consequence of the stabilizing interaction at the interface, and despite opposing the natural depression in free particles this effect is well reproduced by thermodynamical models.[100] Similar measurements have been conducted on bimetallic Pb-Sn[101] and Pb-Bi[102] particles embedded in matrices with different crystalline order, the key role of the interface with the matrix being again emphasized. So far atomistic simulations of such experiments have been rather limited[103,104] and to our best knowledge not extended to nanoalloys.

7 Phase diagrams

The determination of entire phase diagrams, or even parts of diagrams, implies that the relative stabilities of the various phases differing in chemical or structural order be determined as a continuous function of both composition and temperature. In nanoparticles, size is the third key variable and an increasing number of groups have attempted to measure or calculate size-dependent phase diagrams of bimetallic nanoalloys, and even occasionally to delineate three-dimensional diagrams in size, composition and temperature.[72]

It is usually difficult to vary arbitrarily the composition in experiments and molecular dynamics simulations, but this limitation is circumvented in theoretical models based on classical thermodynamics or statistical approaches in grand-canonical ensembles.

Lattice-based studies to address order-disorder transitions are convenient to locate the various equilibrium phases at low temperature, taking into account the specific finite-size effects of surface segregation. One natural advantage of such approaches is that they can be parametrized to reproduce the bulk phase diagram and include some surface properties, hence they have some built-in transferability when addressing nanoscale properties. An example of such approaches is the work by Pohl and coworkers[105] who modeled composition-dependent ordered alloys in Pt-Rh particles and were able to locate the stability regions of the "40" and DO_{22} intermetallic and the solid solution phase as a continuous function of temperature based on Cowley order parameters. In this work SGC Monte Carlo simulations were combined with free-energy integration in order to locate the boundaries between the different phases. The diagrams obtained for three Wulff particles of 807, 2075, or 9201 atoms (diameters of 3.1, 4.3, and 7.8 nm, respectively) are reproduced in Fig. 9. The diagrams show some general decrease in the transition temeprature to the disordered phase, some broadening of the compositional stability range of the ordered phases, but also some less obvious composition-dependence of the boundaries between the ordered phases, including some narrowing of the two-phase regions. In addition, a clear trend for surface segregation of
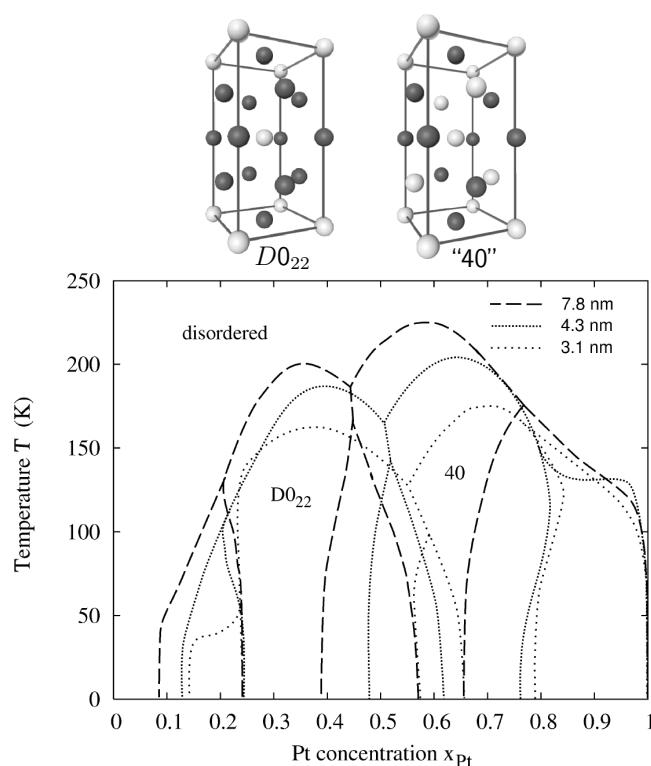

Fig. 9 (Color online) Finite-size phase diagram of Pt-Rh nanoalloy particles containing 807 (3.1 nm), 2075 (4.3 nm) and 9201 (7.8 nm) atoms, as predicted by lattice-based Monte Carlo simulations. The unit cells of the stable intermetallics $D0_{22}$ and "40" are also depicted. [Adapted from J. Pohl, C. Stahl and K. Albe, Size-dependent phase diagrams of metallic alloys: A Monte Carlo simulation study on order-disorder transitions in Pt-Rh nanoparticles, *Beilstein J. Nanotech.*, 2012, **3**, 1-11.]

platinum was found to decrease with increasing platinum concentration, concomitantly with the formation of an ordered alloy in the core.[105]

Off-lattice simulations in the canonical ensemble have been employed to evaluate finite-temperature properties of various phases, fixing temperature, size and composition but comparing different phases in terms of internal energy or enthalpy. Liu and coworkers[106] could thus show that Pt-Au nanoparticles should be more stable against thermal heating in Pt_{core}-Au_{shell} form. Martinez de la Hoz *et al.* similarly confirmed that copper-silver should indeed be more stable as Cu_{core}-Ag_{shell} near room temperature and they evaluated the mixing enthalpy ΔH_{mix} necessary to bring a fully phase separated particle into a random alloy.[107] In particular they verified that ΔH_{mix} satisfies the linear dependence in $1/R$ predicted by classical thermodynamical models.[108]

The interplay between phase segregation and global chemical ordering was similarly simulated by Wang and Hou[109]

for the Pt-Au system. By employing a semiempirical potential reproducing fairly well the bulk phase diagram, a small but representative Wulff nanoparticle of 586 atom was found to undergo various transformations upon increasing its platinum concentration through the Au-rich (α') and Pt-rich (α'') phases. The phase diagram for this nanoparticle, sketched in Fig. 10, exhibits distinct phase separation patterns that originate from the presence of the free surface. At low platinum
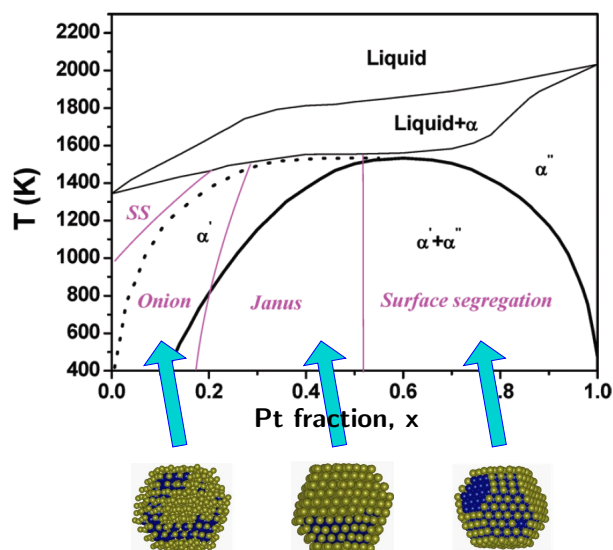

Fig. 10 (Color online) Simulated phase diagram of Au-Pt nanoalloys obtained using an analytical potential and an off-lattice description. Typical patterns exhibitted by the system in different regions of the phase diagram. [Adapted with permission from Y. Wang and M. Hou, Ordering of bimetallic nanoalloys predicted from bulk alloy phase diagrams, *J. Phys. Chem. C*, **116**, 10814-10818. Copyright (2012) American Chemical Society.]

fraction, the Pt atoms tend to occupy subsurface sites, giving a distinct onion-ring character to the particle. At higher concentrations the distribution of platinum atoms undergoes an anisotropic transition towards a core/shell shape with a strongly off-center, Janus-like phase. As the Pt fraction further increases, the core/shell phase separation becomes increasingly isotropic and platinum eventually emerges to the outer layer. Temperature effects were also found to be quite significant, favoring the isotropic onion-ring configurations over the Janus shape for some compositions. Although the authors did not address the melting transition in itself, the stability regions of the various phase separated phases could be evaluated with a good accuracy, not only for the Pt-Au case but also, in the same work, for copper-nickel and gold-cobalt particles.[109]

Several nanoscale phase diagrams of miscible alloys have been studied as well. Copper-nickel, in particular, has received sustain attention from the perspective of classical ther-

modynamical modeling[110,111] and experiment as well.[111] The phase diagrams near the melting region independently obtained by Shirinyan and coworkers[110] for 30-nm particles and by Sopousek *et al.*[111] for 5- and 10-nm particles are reproduced in Fig. 11(a) and (b), respectively. The predictions of both groups are consistent for the decrease in solidus and liquidus temperatures in the whole composition range, however they differ with respect to the solubility propensity. In the CALPHAD-based calculation of Sopousek and coworkers,[111] finite-size effects barely modify the stability range separating the solidus and liquidus lines (except for a global shift to lower temperatures). In contrast, the modeling of Shirinyan *et al.* takes also depletion effects into account,[30] or the requirement of a minimum amount of matter for the transition to take place, which leads to narrowing the two-phase region. Interestingly, DSC measurements performed by Sopousek *et al.*[111] have reported distinct solidus and liquidus temperatures at the composition close to 12% nickel, for particles significantly smaller than 30 nm. This could indicate that the depletion effect included by Shirinyan and coworkers[110] may have been overestimated in this system, however those authors also noticed that kinetic effects may be important and contribute to stabilizing the two-phase region dramatically owing to large nucleation barriers.

Guisbiers and coworkers[90] have recently combined different computational and experimental methods to determine the phase diagram of gold-copper nanoalloys. This system exhibits a congruent melting point near equiconcentration where the bimetallic system behaves as a pure element. A classical thermodyamic model was constructed for solid particles with different symmetries, using the knowledge of surface energies of specific crystalline facets and within the approximation of a regular solution model. The phase diagram predicted in this work revealed significant dependence on size but also on the shape of the particles, chemical order being of the core/shell type with some surface segregation of gold. Such effect were supported by molecular dynamics simulations and high-resolution electron microscopy measurements. The model also predicts a systematic shift of the congruent concentration at higher copper concentrations as the particle size is decreased.[90]

8 Concluding remarks

The equilibrium thermodynamics of nanoalloys, as presented in the previous pages, remains a relatively novel field with many common issues general to the physics and chemistry of nanoscale objects. In particular, its squarely confronts the duality between the macroscopic perspective adopted for larger particles in the scalable regime and the atomistic approach more suitable in smaller clusters dominated by strong finite-size effects. This duality is present among theoreticians who
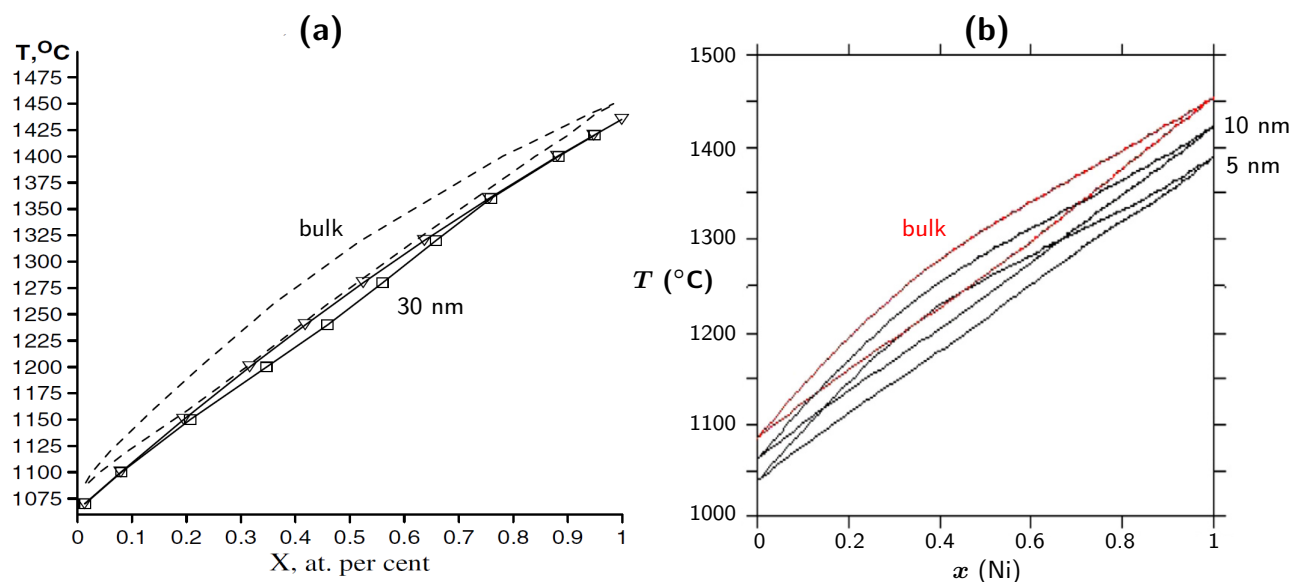
Fig. 11 (Color online) Theoretical solubility diagrams of Cu-Ni nanoalloys computed using mesoscopic approaches. (a) Diagram obtained for particles of 30 nm diameter (symbols) and compared to the bulk diagram (dashed lines). [Adapted with permission from A. Shirinyan, M. Wautelet and Y. Belogorodsky, Solubility diagram of the Cu-Ni nanosystem, *J. Phys.: Condens. Matt.*, **18**, 2537-2551. Copyright (2006) Institute of Physics.] (b) Diagram obtained for 5- and 10-nm diameter particles, and compared to the bulk diagram, as predicted by the CALPHAD approach. [Adapted from J. Sopousek, J. Vrestal, J. Pinkas, P. Broz, J. Bursik, A. Styskalik, D. Skoda, O. Zobac and J. Lee, Cu-Ni nanoalloy phase diagram – Prediction and experiment, *CALPHAD*, **45**, 33-39. Copyright (2014) with permission from Elsevier.]

use either classical thermodynamic models to predict size variations of the phase diagram or molecular simulations possibly detailed at the level of electronic structure to get further insight into the mechanisms associated with the various phase changes. It also exists among experimentalists, who can perform nanocalorimetry experiments on large samples of deposited particles of thousands to millions of atoms, or highly detailed evaluations of entire caloric curves for size-selected clusters at the atomic resolution.

In most investigations these two complementary perspectives are ignored from one another because the systems they deal with are not considered to really overlap. While they aim to capture different elements of complexity, their objects of study actually differ only in size, and often not by so much. From a fundamental point of view, bridging those approaches would be invaluable in order to determine the onset of the scalable regime. As far as modeling is concerned, and with advances in algorithms and computer hardware, this objective should be realistic and successful, hopefully providing in the next few years a more global but still quantitative picture of the factors responsible for phase transformation in medium-size nanoalloys. The validity range of macroscopic approaches and the determination of finite-size parameters that are difficult to evaluate from experiment or ab initio theory alone are two examples where atomistic simulation can provide such valuable insight, as illustrated recently on the calculation of the Tolman

length of nanoalloys which corrects the surface tension from leading-order curvature effects.[112] Experimentally the situation is not as clear, because nanocalorimetry measurements on large particles would be plagued by the problem of size dispersion in smaller systems, while measurements on small size-selected clusters cannot be easily upscaled to very large sizes.

Besides such intrinsic limitations, and in view of their relevance in experiments and future practical applications, it would be desirable to incorporate more realistically the effects of the environment (surfactants, deposition on a substrate or embedding in a solid or porous matrix) in the theoretical models of all kinds. Finally, one aspect of thermodynamics applied to nanoalloys remains to be evoked, in relation with kinetics and kinetic stability. One strong motivation behind nanoalloys is driven by the experimental ability to synthesise very diverse structures and shapes, especially with colloidal reduction chemical techniques,[3–7] where particles similar in size and composition can be produced under different chemical order ranging from core-shell or reverse core-shell to random alloy depending on the details of the synthesis protocol. The fabrication of metastable nanoalloys raises fundamental and very practical issues at the same time. Particles produced out of thermal equilibrium will evolve over time to different structures that have lower free energy. However, for applications it is necessary that this relaxation time is as long as

possible, much longer at least than the capabilities of direct molecular dynamics simulations. Investigations of the kinetics in nanoalloys are rather scarce, although some measurements have provided evidence for chemical reordering in miscible nanoparticles.[113–115] Circumventing the limited time scales of atomistic simulations is possible by using rate theories, and only recently such approaches have been applied to the rearrangement kinetics in model nanoalloys.[116,117]

By construction, and although some authors have discussed the kinetics of phase transformation in relation to the time needed to cross the nucleation barrier,[110] classical thermodynamic models assume thermal equilibrium and are unable to describe particles explicitly prepared in metastable states. Molecular simulation, on the other hand, can simulate arbitrary systems even away from their known low-energy structure. The use of ergodic methods such as replica-echange Monte Carlo should, if properly converged, alleviate the dependence of the results on the initial conditions of the simulation, providing in principle results that reflect the true equilibrium thermodynamics. However such methods would not be appropriate to study metastable systems, and regular molecular dynamics would seem preferable then. While the MD approach has been employed in non-equilibrium situations on several occasions,[106,118] the predicted properties should not be mistaken as reflecting the intrinsic thermal state of the truely equilibrated system. At the very best, the transition temperatures evaluated from such non-equilibrium models should underestimate the onset of the transition at equilibrium,[119] although it is in general difficult to extrapolate short-time data to macroscopic durations.

References

1 R. Busani, M. Folkers and O. Cheshnovsky, Direct Observation of Band-Gap Closure in Mercury Clusters *Phys. Rev. Lett.*, 1998, **81**, 3836-3839.

2 G. Wulff, Zur Frage der Geschwindigkeit des Wachstums und der Auflsung von Krystallflchen, *Z. Kristallogr.*, 1901, **34**, 449-530.

3 R. Ferrando, J. Jellinek and R. L. Johnston, Nanoalloys: From theory to applications of alloy clusters and nanoparticles, *Chem. Rev.*, 2008, **108**, 845-910.

4 D. Alloyeau, C. Mottet and C. Ricolleau, *Nanoalloys: synthesis, structure and properties*, Engineering Materials (Springer, London, 2012).

5 R. L. Johnston and J. P. Wilcoxon, *Metal nanoparticles and nanoalloys*, Frontiers of Nanoscience vol 3 (Elsevier, Oxford, 2012).

6 F. Calvo, *Nanoalloys: from fundamentals to emergent applications* (Elsevier, Oxford, 2013).

7 M. M. Mariscal, O. Oviedo and E. P. M. Lieva, *Metal Clusters and Nanoalloys*, Nanostructure Science and Technology (Springer, New York, 2013).

8 J. Jortner, Cluster size effects, *Z. Phys. D: At. Mol. Clusters*, 1992, **24**, 247-275.

9 see e.g. U. Mizutani, *Hume-Rothery rules for structurally complex alloy phases* (CRC Press, Boca Raton FL, 2011).

10 M. P. Andrews and S. C. O'Brien, Gas-phase "molecular alloys" of bulk immiscible elements: iron-silver (Fe_xAg_y), *J. Phys. Chem.*, 1992, **96**, 8233-8241.

11 T. Wen and K. Krishnan, Thermal stability and morphological transformations of Au_{core}–Co_{shell} nanocrucibles, *J. Phys. Chem. C*, 2010, **114**, 14838-14842.

12 M. H. Ghatee and K. Shekoohi, Structures, thermal stability, and melting behaviors of bimetallic Cs-Na clusters studied via molecular dynamics simulations, *Fluid Phase Eq.* 2013, **355**, 114-122.

13 F. Delogu, Demixing phenomena in NiAl nanometre-sized particles, *Nanotechnology*, 2007, **18**, 065708.

14 F. Delogu, The mechanism of chemical disordering in Cu_3Au nanometre-sized systems, *Nanotechnology*, 2007, **18**, 235706.

15 F. Baletto and R. Ferrando, Structural properties of nanoclusters: Energetic, thermodynamic, and kinetic effects, *Rev. Mod. Phys.* 2005, **77**, 371-423.

16 J. P. K. Doye and F. Calvo, Entropic effects on the size dependence of cluster structure, *Phys. Rev. Lett.*, 2001, **86**, 3570-3573.

17 D. Alloyeau, G. Prévot, Y. Le Bouar, T. Oikawa, C. Langlois, A. Loiseau and C. Ricolleau, Ostwald Ripening in nanoalloys: When thermodynamics drives a size-dependent particle composition, *Phys. Rev. Lett.*, 2010, **105**, 255901.

18 T. L. Hill, *Thermodynamics of small systems* (Dover, NY, 1994).

19 A. Aguado and M. F. Jarrold, Melting and freezing of metal clusters, *Annu. Rev. Phys. Chem.*, 2011, **62**, 151-172.

20 G. M. Wang, E. M. Sevick, E. Mittag, D. J. Searles, and D. J. Evans. Experimental demostration of violations of the second law of thermodynamics for small systems and short time scales, *Phys. Rev. Lett.*, 2002, **89**, 050601.

21 C. N. Yang and T. Lee, Statistical theory of equations of state and phase transitions. I. Theory of condensation, *Phys. Rev.*, 1952, **87**, 404-409.

22 P. Labastie and R. L. Whetten, Statistical thermodynamics of the cluster solid-liquid transition, *Phys. Rev. Lett.*, 1990, **65**, 1567-1570.

23 A. S. Shirinyan and M. Wautelet, Phase separation in nanoparticles, *Nanotechnology*, 2004, **15**, 1720-1731.

24 P. Pawlaw, Über die abhängigkeit des schmelzpunktes von der oberflächenergie eines festen körpers, *Z. Phys. Chem.*, 1909, **65**, 1-35.

25 Ph. Buffat and J.-P. Borel, Size effect on the melting temperatures of gold particles, *Phys. Rev. A*, 1976, **13**, 2287-2298.

26 E. Pahl, F. Calvo, L. Koči, and P. Schwerdtfeger, Accurate melting temperatures for neon and argon from ab initio Monte Carlo simulations, *Angew. Chem. Int. Ed.*, 2008, **47**, 8207-8210.

27 H. H. Farrell and C. D. Van Siclen, Binding energy, vapor pressure, and melting point of semiconductor nanoparticles, *J. Vac. Sci. Technol. B*, 2007, **25**, 1441-1447.

28 R. S. Berry, J. Jellinek and G. Natanson, Unequal freezing and melting temperatures for clusters, *Chem. Phys. Lett.*, 1984, **107**, 227-230.

29 Y. Imry, Finite-size rounding of a first-order phase transition, *Phys. Rev. B*, 1980, **21**, 2042-2043.

30 A. S. Shirinyan, A. M. Gusak and M. Wautelet, Phase diagram versus diagram of solubility: What is the difference for nanosystems? *Acta Mater.*, 2005, **53**, 5025-5032.

31 S. L. Lai, J. Y. Guo, V. Petrova, G. Ramanath, and L. H. Allen, Size-dependent melting properties of small tin particles: nanocalorimetric measurements, *Phys. Rev. Lett.*, 1996, **77**, 99-102.

32 F. Calvo and P. Labastie, Evidence for surface melting in clusters made of double icosahedron units, *Chem. Phys. Lett.*, 1996, **258**, 233-238.

33 J. P. K. Doye and D. J. Wales, Thermodynamics of global optimization, *Phys. Rev. Lett.* 1998, **80**, 1357-1360.

34 G. A. Breaux, C. M. Neal, B. Cao and M. F. Jarrold, Melting, premelting, and structural transitions in size-selected aluminum clusters with around 55 atoms, *Phys. Rev. Lett.*, 2005, **94**, 173401.

35 B. Cao, A. K. Starace, C. M. Neal, M. F. Jarrold, S. Núñez, J. M. López and A. Aguado, Substituting a copper atom modifies the melting of aluminum clusters, *J. Chem. Phys.*, 2008, **129**, 124709.

36 G. A. Breaux, R. C. Benirschke, T. Sugai, B. S. Kinnear and M. F. Jarrold,

Hot and solid gallium clusters: too hot to melt, *Phys. Rev. Lett.*, 2003, **91**, 215508.

37 Z. L. Wang, J. M. Petroski, T. C. Green, and M. A. El-Sayed, Shape Transformation and surface melting of cubic and tetrahedral platinum nanocrystals, *J. Phys. Chem. B*, 1998, **102**, 6145-6151.

38 M. Maier-Borst, D. B. Cameron, M. Rokni and J. H. Parks, Electron diffraction of trapped ions, *Phys. Rev. A*, 1999, **59**, R3162-R3165.

39 J. P. Butler, Thermodynamics of the surfaces of solutions, *Proc. Roy. Soc. London A*, 1932, **135**, 348-375.

40 L. Kaufman and H. Bernstein, Computer Calculation of Phase Diagrams (Academic Press, New York), 1970.

41 J. Lee, J. Park, and T. Tanaka, Effects of interaction parameters and melting points of pure metals on the phase diagrams of the binary alloy nanoparticle systems: A classical approach based on the regular solution model, *CALPHAD*, 2009, **33**, 377-381.

42 G. Geyer, in *Computing Science and Statistics: Proceedings of the 23rd Symposium on the Interface*, edited by E. K. Keramidas (Interface Foundation, Fairfax Station, 1991), p. 156.

43 Y. Sugita and Y. Okamoto, Replica-exchange molecular dynamics method for protein folding, *Chem. Phys. Lett.*, 1999, **314**, 141-151.

44 F. Wang and D. P. Landau, Efficient, multiple-range random walk algorithm to calculate the density of states, *Phys. Rev. Lett.*, 2001, **86**, 2050-2053.

45 L. Piccolo, A. Piednoir, and J.-C. Bertolini, Pd-Au single-crystal surfaces: Segregation properties and catalytic activity in the selective hydrogenation of 1,3-butadiene, *Surf. Sci.*, 2005, **592**, 169-181.

46 L. Hilaire, P. Légaré, Y. Holl and G. Maire, Interaction of oxygen and hydrogen with Pd-Au alloys - An AES and XPS study, *Surf. Sci.*, 1981, **103**, 125-140.

47 I. Atanasov and M. Hou, Equilibrium ordering properties of Au-Pd alloys and nanoalloys, *Surf. Sci.*, 2009, **603**, 2639-2651.

48 P. Lu, M. Chandross, T. J. Boyle, B. G. Clark and P. Vianco, Equilibrium Cu-Ag nanoalloy structure formation revealed by *in situ* scanning transmission electron microscopy heating experiments, *APL Mat.*, 2014, **2**, 022107.

49 L. Delfour, J. Creuze, and B. Legrand, Exotic behavior of the outer shell of bimetallic nanoalloys, *Phys. Rev. Lett.*, 2009, **103**, 205701.

50 L. Fiermans, R. D. Gryse, G. D. Doncker, Pd segregation to the surface of bimetallic Pt-Pd particles supported on H-beta zeolite evidenced with X-ray photoelectron spectroscopy and argon cation bombardment, P. A. Jacobs and A. J. Martens, *J. Catal.*, 2000, **193**, 108-114.

51 U. Kolb, S. A. Quaiser, M. Winter and M. T. Reetz, Investigation of tetraalkylammonium bromide stabilized palladium/platinum bimetallic clusters using extended X-ray absorption fine structure spectroscopy, *Chem. Mater.*, 1996, **8**, 1889-1894.

52 G. Barcaro, A. Fortunelli, M. Polak and L. Rubinovich, Patchy multishell segregation in Pd-Pt alloy nanoparticles, *Nano Lett.*, 2011, **11**, 1766-1769.

53 F. Calvo, Solid-solution precursor to melting in onion-ring Pd-Pt nanoclusters: a case of second-order-like phase change?, *Faraday Discuss.*, 2008, **138**, 75-88.

54 B. J. Hwang, L. S. Sarma, J. M. Chen, C. H. Chen, S. C. Shih, G. R. Wang, D. G. Liu, J. F. Lee and M. T. Tang, Structural models and atomic distribution of bimetallic nanoparticles as investigated by X-ray absorption spectroscopy, *J. Am. Chem. Soc.*, 2005, **127**, 11140-11145.

55 L. Rubinovich and M. Polak, Prediction of distinct surface segregation effects due to coordination-dependent bond-energy variations in alloy nanoclusters, *Phys. Rev. B*, 2009, **80**, 045404.

56 M. Polak and L. Rubinovich, The interplay of surface segregation and atomic order in alloys, *Surf. Sci. Rep.*, 2000, **138**, 127-194.

57 L.-L. Wang, T. L. Tan and D. J. Johnson, Nanoalloy composition-temperature phase diagram for catalyst design: Case study of Ag-Au, *Phys. Rev. B*, 2012, **86**, 035438.

58 J. M. Sanchez, F. Ducastelle and D. Gratias, Generalized cluster description of multicomponent systems, *Physica A: Stat. Mech. Appl.*, 1984, **128**, 334-350.

59 L.-L. Wang, T. L. Tan and D. J. Johnson, Configurational thermodynamics of alloyed nanoparticles with adsorbates, *Nano Lett.*, 2014, **14**, 7077-7084.

60 J. R. Renzas, W. Y. Huang, Y. W. Zhang, M. E. Grass, D. T. Hoang, S. Alayoglu, D. R. Butcher, F. Tao, Z. Liu and G. A. Somorjai, *Phys. Chem. Chem. Phys.*, 2011, **13**, 2556-2562.

61 I. M. L. Billas, J. A. Becker, A. Chatelain and W. A. de Heer, Magnetic moments of iron clusters with 25 to 700 atoms and their dependence on temperature, *Phys. Rev. Lett.*, 1993, **71**, 4067-4070.

62 K. Sato, B. Bian and Y. Hirotsu, Fabrication of oriented $L1_0$-FePt and FePd nanoparticles with large coercivity, *J. Appl. Phys.*, 2002, **91**, 8516-8518.

63 M. Müller and K. Albe, Lattice Monte Carlo simulations of FePt nanoparticles: Influence of size, composition and surface segregation on order-disorder phenomena, *Phys. Rev. B*, 2005, **72**, 094203.

64 R. V. Chepulskii and W. H. Butler, Temperature and particle-size dependence of the equilibrium order parameter of FePt alloys, *Phys. Rev. B*, 2005, **72**, 134205.

65 B. Yang, M. Asta, O. N. Mryasov, T. J. Klemmer and R. W. Chantrell, The nature of A1-$L1_0$ ordering transitions in alloy nanoparticles: A Monte Carlo study, *Acta Mater.*, 2006, **54**, 4201-4211.

66 F. Tournus, A. Tamion, N. Blanc, A. Hannour, L. Bardotti, B. Prével, P. Ohresser, E. Bonet, T. Epicier and V. Dupuis, Evidence of $L1_0$ chemical order in CoPt nanoclusters: Direct observation and magnetic signature, *Phys. Rev. B*, 2008, **77**, 144411.

67 D. Alloyeau, C. Ricolleau, C. Mottet, T. Oikawa, C. Langlois, Y. Le Bouar, N. Braidy, and A. Loiseau, Size and shape effects on the order-disorder phase transition in CoPt nanoparticles, *Nature Mat.*, 2009, **8**, 940-946.

68 F. Calvo and C. Mottet, Order-disorder transition in Co-Pt nanoparticles: Coexistence, transition states and finite-size effects, *Phys. Rev. B*, 2011, **84**, 035409.

69 C. Goyhenex, H. Bullou, J.-P. Deville and G. Tréglia, Pt/Co(0001) superstructures in the sub;onolayer range: A tight-binding quenched molecular dynamics study, *Phys. Rev. B*, 1999, **60**, 2781-2788.

70 J. M. Cowley, An approximate theory of order in alloys, *Phys. Rev.*, 1950, **77**, 669-675.

71 W. Qi, Y. Li, S. Xiong and S.-T. Lee, Modeling size and shape effects on the order-disorder phase-transition temperature of CoPt nanoparticles, *Small*, 2010, **6**, 1996-1999.

72 W. A. Jesser, R. Z. Schneck, and W. W. Gile, Solid-liquid equilibria in nanoparticles of Pb-Bi alloys, *Phys. Rev. B*, 2004, **69**, 144121.

73 C. L. Chen, J.-G. Lee, K. Arakawa and H. Mori, Quantitative analysis on size dependence of eutectic temperature of alloy nanoparticles in the Ag-Pb system, *Appl. Phys. Lett.*, 2011, **98**, 083108.

74 C. Hock, S. Strassburg, H. Haberland, B. von Issendorff, A. Aguado and M. Schmidt, Melting-point depression by insoluble impurities: a finite-size effect, *Phys. Rev. Lett.*, 2008, **101**, 023401.

75 C. Mottet, G. Rossi, F. Baletto, and R. Ferrando, Single impurity effect on the melting of nanoclusters, *Phys. Rev. Lett.*, 2005, **95**, 035501.

76 J. Jellinek and E. B. Krissinel, Ni_nAl_m alloy clusters: analysis of structural forms and their energy ordering, *Chem. Phys. Lett.*, 1996, **258**, 283-292.

77 D. J. Wales, *Energy Landscapes* (Cambridge University Press, Cambridge, 2003).

78 M. Brack, The physics of simple metal clusters: self-consistent jellium model and semiclassical approaches, *Rev. Mod. Phys.*, 1993, **65**, 677-732.

79 F. Calvo, E. Cottancin, and M. Broyer, Segregation, core alloying, and shape transitions in bimetallic nanoclusters: Monte Carlo simulations, *Phys. Rev. B*, 2008, **77**, 121406(R).

80 E. Cottancin, M. Gaudry, M. Pellarin, J. Lermé, L. Arnaud, J. R. Huntzinger, J.-L. Vialle, M. Treilleux, P. Mélinon, J.-L. Rousset and M.

Broyer, Optical properties of mixed clusters: comparative study of Ni/Ag and Pt/Ag clusters, *Eur. Phys. J. D*, 2003, **24**, 111-114.

81 T. B. Massalski, J. L. Murray, L. H. Bernett and H. Baker, *Binary Alloy Phase Diagrams* (American Society for Metals, Metals Park, OH, 1986), vol. 1.

82 D. Bochicchio and R. Ferrando, Morphological instability of core-shell metallic nanoparticles, *Phys. Rev. B*, 2013, **87**, 165435.

83 M. Cazayous, C. Langlois, T. Oikawa, C. Ricolleau, and A. Sacuto, Confocal Raman and TEM measurement at the same area on nanoparticles, *Microelectron. Eng.*, 2007, **84**, 419-423.

84 H. Y. Oderji, H. Behnejad, R. Ferrando and H. Ding, System-dependent melting behavior of icosahedral anti-Mackay nanoalloys, *RSC Adv.*, 2013, **3**, 21981-21993.

85 D. Palagin and J. P. K. Doye, Ni-based nanoalloys: Towards thermally stable highly magnetic materials, *J. Chem. Phys.*, 2014, **141**, 214302.

86 A. Aguado and J. M. López, Structural and thermal behavior of compact core-shell nanoparticles: Core instabilities and dynamic contributions to surface thermal stability, *Phys. Rev. B*, 2005, **72**, 205420.

87 U. Ojha, K. G. Steenbergen, and N. Gaston, How a single aluminum atom makes a difference to gallium: First-principles simulations of bimetallic cluster melting, *J. Chem. Phys.*, 2013, **139**, 094309.

88 Z. Yang, X. Yang, and Z. Xu, Molecular dynamics simulation of the melting behavior of Pt-Au nanoparticles with core-shell structure, *J. Phys. Chem. C*, 2008, **112**, 4937-4947.

89 R. Huang, Y.-H. Wen, G.-F. Shao, and S.-G. Sun, Insight into the melting behavior of Au-Pt core-shell nanoparticles from atomistic simulations, *J. Phys. Chem. C*, 2013, **117**, 4278-4286.

90 G. Guisbiers, S. Mejia-Rosales, S. Khanal, F. Ruiz-Zepeda, R. L. Whetten and M. José-Yacaman, Gold-copper nano-alloy, "*Tumbaga*", in the era of nano: phase diagram and segregation, *Nano Lett.*, 2014, **14**, 6718-6726.

91 A. Rapallo, J. A. Olmos-Asar, O. A. Oviedo, M. Ludueña, R. Ferrando and M. M. Mariscal, Thermal properties of Cu/Au nanoalloys and comparison of different computer simulation techniques, *J. Phys. Chem. C*, 2012, **116**, 17210-17218.

92 F. Chen and R. L. Johnston, Energetic, electronic, and thermal effects on structural properties of Ag-Au nanoalloys, *ACS Nano*, 2008, **2**, 165-175.

93 S. P. Huang, D. Mainardi and P. Balbuena, Structure and dynamics of graphite-supported bimetallic nanoclusters, *Surf. Sci.*, 2003, **545**, 163-179.

94 S. K. R. S. Sankaranarayanan, V. R. Bhethanabotla and B. Joseph, Molecular dynamics simulations of the structural and dynamic properties of graphite-supported bimetallic transition metal clusters, *Phys. Rev. B*, 2005, **72**, 195405.

95 J. Mu, Z. W. Zhu, H. F. Zhang, H. M. Fu, A. M. Wang, H. Li, Z. Q. Hu, Size dependent melting behaviors of nanocrystalline particles embedded in amorphous matrix, *J. Appl. Phys.*, 2012, **111**, 043515.

96 H. Saka, Y. Nishikawa, and T. Imura, Melting temperature of In particles embedded in an Al matrix, *Philos. Mag. A*, 1988, **57**, 895-906.

97 H. W. Sheng, G. Ren, L. M. Peng, Z. Q. Hu and K. Lu, Superheating and melting-point depression of Pb nanoparticles embedded in Al matrices, *Phil. Mag. Lett.*, 1996, **73**, 179-186.

98 J. Zhong, L. H. Zhang, Z. H. Jin, M. L. Sui and K. Lu, Superheating of Ag nanoparticles embedded in Ni matrix, *Acta. Mater.*, 2001, **49**, 2897-2904.

99 O. A. Yeshchenko, I. M. Dmitruk, A. A. Alexeenko and A. M. Dmytruk, Size-dependent melting of spherical copper nanoparticles embedded in a silica matrix, *Phys. Rev. B*, 2007, **75**, 085434.

100 K. K. Nanda, S. N. Sahu and S. N. Behera, Liquid-drop model for the size-dependent melting of low-dimensional systems, *Phys. Rev. A*, 2002, **66**, 013208.

101 P. Y. Khan and K. Biswas, The effect of matrix on melting and solidification behaviours of embedded Pb-Sn alloy nanopartices, *Philos. Mag.*, 2014, **94**, 2031-2045.

102 P. Y. Khan and K. Biswas, Melting and solidification behaviour of

Bi-Pb multiphase alloy nanoparticles embedded in aluminum matrix, *J. Nanosci. Nanotechnol.*, 2015, **15**, 309-316.

103 F. Celestini, R. J. M. Pellenq, P. Bordarier and B. Rousseau, Melting of Lennard-Jones clusters in confined geometries, *Z. Phys. D: At. Mol. Clusters*, 1996, **37**, 49-53.

104 Z. H. Jin, H. W. Sheng, and K. Lu, Melting of Pb clusters without free surfaces, *Phys. Rev. B*, 1999, **60**, 141-149.

105 J. Pohl, C. Stahl and K. Albe, Size-dependent phase diagrams of metallic alloys: A Monte Carlo simulation study on order-disorder transitions in Pt-Rh nanoparticles, *Beilstein J. Nanotech.*, 2012, **3**, 1-11.

106 H. B. Liu, U. Pal and J. A. Asciencio, Thermodynamic stability and melting mechanism of bimetallic Au-Pt nanoparticles, *J. Phys. Chem. C*, 2008, **112**, 19173-19177.

107 J. M. Martinez De La Hoz, R. Callejas Tovar and P. B. Balbuena, Size effect on the stability of Cu-Ag nanoalloys, *Molec. Sim.*, 2009, **35**, 785-794.

108 S. Xiao, W. Hu, W. Luo, Y. Wu, X. Li, and H. Deng, Size effect on the alloying ability and phase stability of immiscible bimetallic nanoparticles, *Eur. Phys. J. B*, 2006, **54**, 479-484.

109 Y. Wang and M. Hou, Ordering of bimetallic nanoalloys predicted from bulk alloy phase diagrams, *J. Phys. Chem. C*, 2012, **116**, 10814-10818.

110 A. Shirinyan, M. Wautelet and Y. Belogorodsky, Solubility diagram of the Cu-Ni nanosystem, *J. Phys.: Condens. Matt.*, 2006, **18**, 2537-2551.

111 J. Sopousek, J. Vrestal, J. Pinkas, P. Broz, J. Bursik, A. Styskalik, D. Skoda, O. Zobac and J. Lee, Cu-Ni nanoalloy phase diagram – Prediction and experiment, *CALPHAD*, 2014, **45**, 33-39.

112 F. Calvo, Molecular dynamics determination of the surface tension of silver-gold liquid alloys and the Tolman length of nanoalloys, *J. Chem. Phys.*, 2012, **136**, 154701.

113 H. Yasuda and H. Mori, Effect of cluster size on the chemical ordering in nanometer-sized Au-75at%Cu alloy clusters, *Z. Phys. D: At. Mol. Clusters*, 1996, **31**, 181-186.

114 T. Shibata, B. A. Bunker, Z. Zhang, D. Meisel, C. F. Vardeman, and K. D. Gezelter, Size-dependent spontaneous alloying of Au-Ag nanoparticles, *J. Am. Chem. Soc.*, 2002, **124**, 11989-11996.

115 M. S. Shore, J. Wang, A. C. Johnston-Peck, A. L. Oldenburg, and J. B. Tracy, Synthesis of Au(core)/Ag(shell) nanoparticles and their conversion to AuAg alloy nanoparticles, *Small*, 2011, **7**, 230-234.

116 F. R. Negreiros, F. Taherkhani, G. Parsafar, A. Caro, and A. Fortunelli, Kinetics of chemical ordering in a Ag-Pt nanoalloy particle via first-principles simulations, *J. Chem. Phys.*, 2012, **137**, 194302.

117 F. Calvo, A. Fortunelli, F. Negreiros, and D. J. Wales, Kinetics of chemical ordering in Ag-Au and Ag-Ni nanoalloys, *J. Chem. Phys.*, 2013, **139**, 111102.

118 R. Huang, G.-F. Shao, X.-M. Zeng and Y.-H. Wen, Diverse melting modes and structural collapse of hollow bimetallic core-shell nanoparticles: A perspective from molecular dynamics simulations, *Sci. Rep.*, 2014, **4**, 7051.

119 F. Calvo and D. J. Wales, Relaxation of caloric curves on complex potential energy surfaces, *J. Chem. Phys.*, 2008, **128**, 154501.